Geophysical Journal International

Geophys. J. Int. (2011) **184,** 965–973 doi: 10.1111/j.1365-246X.2010.04900.x

The Gouy phase anomaly for harmonic and time-domain paraxial Gaussian beams

Robert L. Nowack and Sribharath M. Kainkaryam

Department of Earth and Atmospheric Sciences, Purdue University, 550 *Stadium Mall Dr., West Lafayette IN* 47907*, USA. E-mail: nowack@purdue.edu*

Accepted 2010 November 16. Received 2010 November 4; in original form 2010 May 17

SUMMARY

The Gouy phase anomaly resulting from the focusing of wave solutions is illustrated using 2-D paraxial Gaussian beams. For harmonic Gaussian beams, this gives rise to a continuous variation of the Gouy phase as a function of propagation distance. This is in contrast to the discontinuous phase anomaly at caustics for ray solutions. However, as the beam-width of a Gaussian beam at a focus gets smaller, the Gouy phase anomaly becomes more concentrated near the focus and approaches that of the ray solution. The Gouy phase for a harmonic Gaussian beam is first illustrated in a homogeneous medium, and then in a quadratic velocity waveguide where the beam can pass through multiple focus points. However for multiple focus points, care must be taken to ensure that the phase remains continuous. Finally, an example is shown of the Gouy phase for a time-domain signal using a Gabor wavelet. This is validated using the finite difference method, and illustrates the progressive phase advance of a time-domain signal modifying the pulse shape with distance. Intuitively, as a wave solution gets 'squeezed' at a focus, it 'squirts' forward by slightly increasing its apparent speed in the propagation direction and modifying the pulse shape. However, this is a phase advance and not a group or energy advance and does not violate causality. Nonetheless, this could potentially influence the interpretation of travel-times using correlation techniques when using sources that generate beamed signals, for example from transducer sources in the laboratory.

Key words: Theoretical seismology; Wave propagation.

1 INTRODUCTION

Gaussian beams are bounded solutions to the wave equation and can be used to model different types of beamed signals, for example from transducers in the laboratory. Gaussian beams can also be used for the superposition and synthesis of other types of wavefields (e.g. Červený *et al.* 1982; Popov 1982; Nowack & Aki 1984). Here we investigate the so-called Gouy phase anomaly for harmonic and time-domain, paraxial Gaussian beams.

For all wave solutions there is an inter-play between the spatial extent of the solution with the range of wavenumbers required to model it. A spatial restriction or 'squeeze' of a wave solution will result in a change in the average wavenumber in the direction of propagation and a corresponding phase anomaly. The phase anomaly for a 3-D spherically converging wave solution was first observed by Gouy (1890a,b), where it was found to be equal to $-\pi$.

In ray theory, there is an abrupt change of phase at a caustic where the ray amplitude is singular. This phase shift can be determined by matching the ray solutions on either side of a caustic (Červený 2001; Chapman 2004). The so-called 'index of the ray trajectory' (Kravtsov & Orlov 1990) counts the number and order of the caustics encountered by the ray to compute the cumulative phase shift. This is also referred to as the KMAH index after the work of Keller (1958), Maslov (1965), Arnold (1967) and Hörmander (1971). In real data, phase shifts due to caustics can be observed between direct and wide-angle reversed branches for triplicated wave arrivals from rapid increases in velocity with depth. As another example, the phase shift between an sS and SS phase, which undergoes a fold caustic, is shown in fig. 9.15 of Aki & Richards (2002). The KMAH index can be related to the continuous Gouy phase for general wave and beam solutions. Paraxial Gaussian beams are approximate wave solutions along rays, which have complex traveltimes and are non-singular at caustics (Popov 2002).

2 GAUSSIAN BEAMS AND THE GOUY PHASE

Exact Gaussian beams can be derived in several ways (Siegman 1986) including the complex source point approach in which an analytic continuation of a point source from a real source location is performed (Deschamps 1971; Felsen 1976). Other approaches to derive Gaussian beams are from a differential equation approach based on the 'paraxial' wave equation, the Huygens-Fresnel

integral with an initial Gaussian amplitude profile, a plane wave expansion approach and solutions to the Helmholtz equation in oblate spheroidal coordinate systems (Siegman 1986).

Although Gaussian beam solutions don't focus to a point, they do narrow to a beam-waist at a range z_0 with a beam-width of $L(z_0)$, where the transverse amplitude decays to $1/e$ of the peak value. For a Gaussian beam in a homogeneous medium, the beam-width as a function of distance z can be expressed as

$$L(z) = L(z_0)\left(1 + \left(\frac{z}{Z_R}\right)^2\right)^{1/2}, \tag{1}$$

where $Z_R = \pi L^2(z_0)/\lambda$ is called the Rayleigh distance and λ is the wavelength (Siegman 1986). At the Rayleigh distance the beam-width equals $\sqrt{2}L(z_0)$ after which the beam begins to diverge. The Gouy phase anomaly $\psi(z)$ for a Gaussian beam in a homogeneous medium can be written as $\psi(z) = -\frac{n}{2}\tan^{-1}(z/Z_R)$, where $n = 1$ in 2-D and $n = 2$ for 3-D. For heterogeneous media, the Gouy phase anomaly with distance will be more complicated. However, the Gouy phase for beams and other wave solutions is a continuous function of propagation distance, in contrast to that for ray solutions.

There have been a number of explanations for the Gouy phase anomaly, including those related to analogies with quantum physics (Simon & Mukunda 1993; Subbarao 1995). However, this requires a specialized background in quantum physics, which is useful but not essential. Boyd (1980) presented a geometric construction for the Gouy phase in terms of lateral beam spread.

Feng & Winful (2001) gave an explanation of the Gouy phase in terms of a shift in the expectation value of the axial wavenumber resulting from an increase in the transverse wavenumber when a beam is focused or confined. Consider a plane wave of frequency ω, speed v and wavenumber k with a magnitude of $\frac{\omega}{v}$. k has three components that are related by

$$k^2 = k_x^2 + k_y^2 + k_z^2. \tag{2}$$

Although the magnitude of k is a constant, the presence of the transverse components reduce the magnitude of the axial component k_z. The effective axial wavenumber across the face of the beam can be defined as

$$\bar{k}_z = k - \frac{\langle k_x^2 \rangle}{k} - \frac{\langle k_y^2 \rangle}{k}, \tag{3}$$

where the expectations $\langle k_x^2 \rangle$and $\langle k_y^2 \rangle$are taken across the beam in the x and y lateral directions. The Gouy phase anomaly can then be

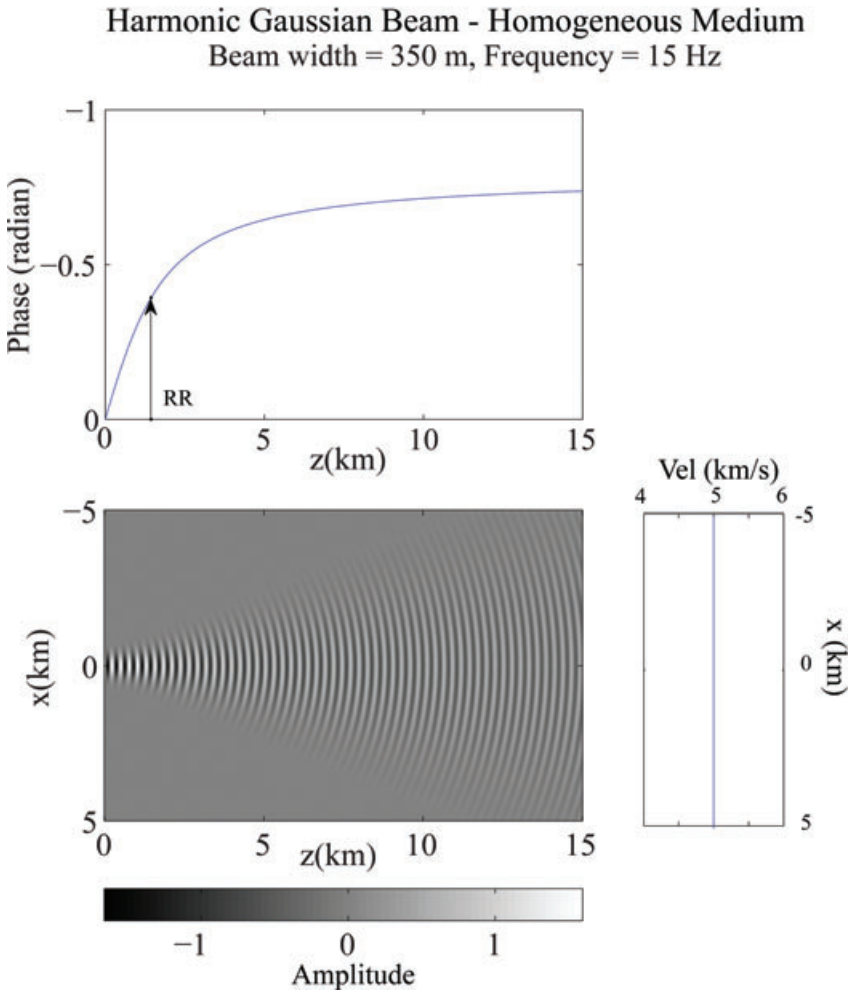

Figure 1. Harmonic Gaussian beam for a frequency of 15 Hz in a homogeneous medium. The beam-waist is at $z = 0$ with a beam-width of 350 m. The beam-field is shown at the bottom and the Gouy phase anomaly at the top. The Rayleigh distance is indicated by RR.

written (Feng & Winful 2001) as

$$\psi(z) = -\frac{1}{k}\int_0^z \left\{\langle k_x^2\rangle + \langle k_y^2\rangle\right\} dz. \tag{4}$$

For a harmonic Gaussian beam in a homogeneous medium, the Gouy phase is $\psi(z) = -(\frac{1}{2} + \frac{1}{2})\tan^{-1}(z/Z_R)$, where Z_R is the Rayleigh range with a $^1/_2$ for each lateral dimension. For $z \to \infty$, then $\psi(z) = -\pi/2$ (with a $-\pi/4$ for each lateral dimension). For a 3-D Gaussian beam, the Gouy phase is progressive from 0 to $-\pi/2$ for distance from the beam waist of $0 < z < \infty$. For 2-D ribbon beams, the phase shift goes from 0 to $-\pi/4$ for $0 < z < \infty$. In Huygens-Fresnel integrals, a $-\pi/2$ phase shift is also required between an incident 3-D wavefront and the 3-D diverging secondary wavelets. For $-\infty < z < +\infty$, the Gouy phase results in a phase shift of $-\pi$ for a 3-D wave ($-\pi/2$ for a 2-D wave) going through a focus and for a Gaussian beam this phase shift is progressive.

To compare with a point or line source solution, in 2-D homogeneous media the wave solution with a singularity at the origin can be written

$$C\, H_0^{(1)}(kr) \sim C\sqrt{\frac{1}{i\,\pi kr}}\, e^{i\,kr},$$

where $H_0^{(1)}(kr)$ is a zero-order Hankel function of the first kind, $r = |x - x_0|$, k is the wavenumber and C is determined from matching the singularity at the origin. The last expression is evaluated for $kr \to \infty$ in the far field and this results in a phase shift of $-\pi/4$ which would be a phase advance with respect to the propagation phase delay term of $+kr$.

For a line source located at the origin, then by matching the singularity at the origin, $C = \frac{i}{4}$ (Chew 1990) and the Green's function can be evaluated in the far field as

$$G(x, x_0) = \frac{i}{4}\, H_0^{(1)}(kr) \sim \sqrt{\frac{1}{8\,\pi\, kr}}\, e^{i\,(kr+\pi/4)}.$$

Thus, for a line source at the origin, this now has a phase delay of $+\pi/4$ with the same sign as the propagation term $+kr$. This is in contrast to the phase shift from a caustic line, or for a 2-D Gaussian beam passing through the beam-waist, which has a phase advance of $-\pi/4$ from $0 \to \infty$ and $-\pi/2$ for waves going from $-\infty \to \infty$. This difference is related to the different boundary conditions on the problem for a wave propagating through a caustic point, in contrast to waves propagating outwards in all directions from a line source.

The Gouy phase described above for a Gaussian beam solution is given for a fundamental mode Gaussian beam. For higher modes in an Hermite-Gaussian beam expansion, the Gouy phase is

$$\psi(z) = -(m + n + 1)\tan^{-1}\left(\frac{z}{Z_R}\right), \tag{5}$$

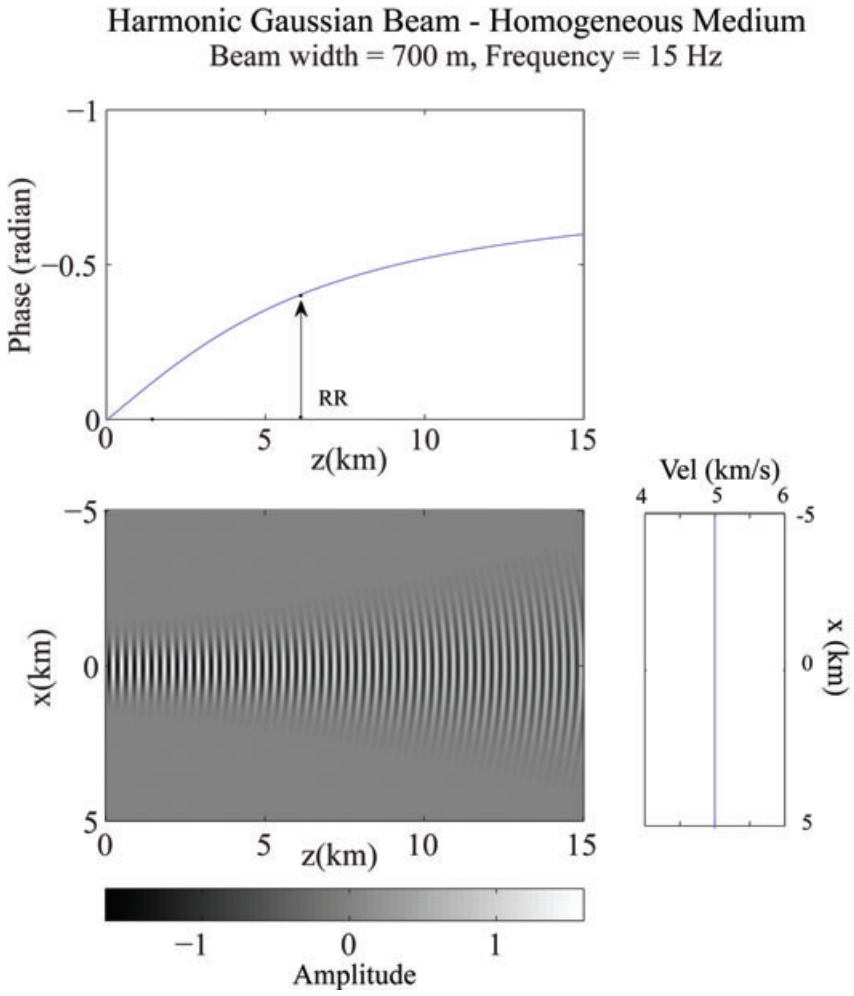

Figure 2. Harmonic Gaussian beam for a frequency of 15 Hz in a homogeneous medium. The beam-waist is at $z = 0$ with a beam-width of 700 m. The beam-field is shown at the bottom and the Gouy phase anomaly at the top. The Rayleigh range is indicated by RR.

where the indices m and n are the mode numbers for the higher order Gaussian beams (Feng & Winful 2001).

Wave solutions, including beams, exhibit a spatial and wavenumber duality where an uncertainty principle results with

$$\Delta k_\rho \Delta \rho \geq \text{constant}, \tag{6}$$

where ρ is a general transverse coordinate and k_ρ is the corresponding transverse wavenumber. As $\Delta\rho$ gets smaller from wave focusing, then Δk_ρ gets bigger resulting in a larger Gouy phase anomaly. However, the phase space taken up by the higher order Gaussian beams is generally larger than for zeroth order beams with a larger constant in the uncertainty relation (Feng & Winful 2001).

3 PARAXIAL GAUSSIAN BEAMS IN 2-D

Approximate paraxial Gaussian beams in inhomogeneous media can be described using dynamic ray tracing with complex initial conditions along a real ray and this provides a major computational advantage for the calculation of high-frequency Gaussian beams in smoothly varying media. Overviews of paraxial Gaussian beams using dynamic ray tracing are given by Kravtsov & Berczynski (2007), Popov (2002), Červený (2001), where the complex part of the eikonal gives rise to a Gaussian amplitude shape.

In 2-D, the ray-centred coordinates are given by (s, n) where s is the coordinate along the ray and n is transverse to the ray. A paraxial Gaussian beam connected with such a central ray is given by (Červený *et al.* 1982)

$$u(s,n,t) = \sqrt{v(s)/q(s)}\,\exp\left\{-i\omega\left(t - \int_{s_0}^{s} ds v^{-1}(s)\right) + i\frac{\omega}{2}\frac{p(s)}{q(s)}n^2\right\}, \tag{7}$$

where $v(s)$ is the velocity along the central ray and $p(s)$ and $q(s)$ are the complex solutions of the dynamic ray equations. These can be constructed by a linear combination of real fundamental solutions of the dynamic ray equations with complex initial conditions. Thus, the complex $p(s)$ and $q(s)$ can be written as

$$\begin{aligned} p(s) &= \varepsilon p_1(s) + p_2(s) \\ q(s) &= \varepsilon q_1(s) + q_2(s), \end{aligned} \tag{8}$$

where $(q_1(s),\ p_1(s))$ and $(q_2(s),\ p_2(s))$ are the fundamental real solutions. ε is the complex beam parameter that specifies the position of the beam waist and the beam-width of the Gaussian beam (Červený

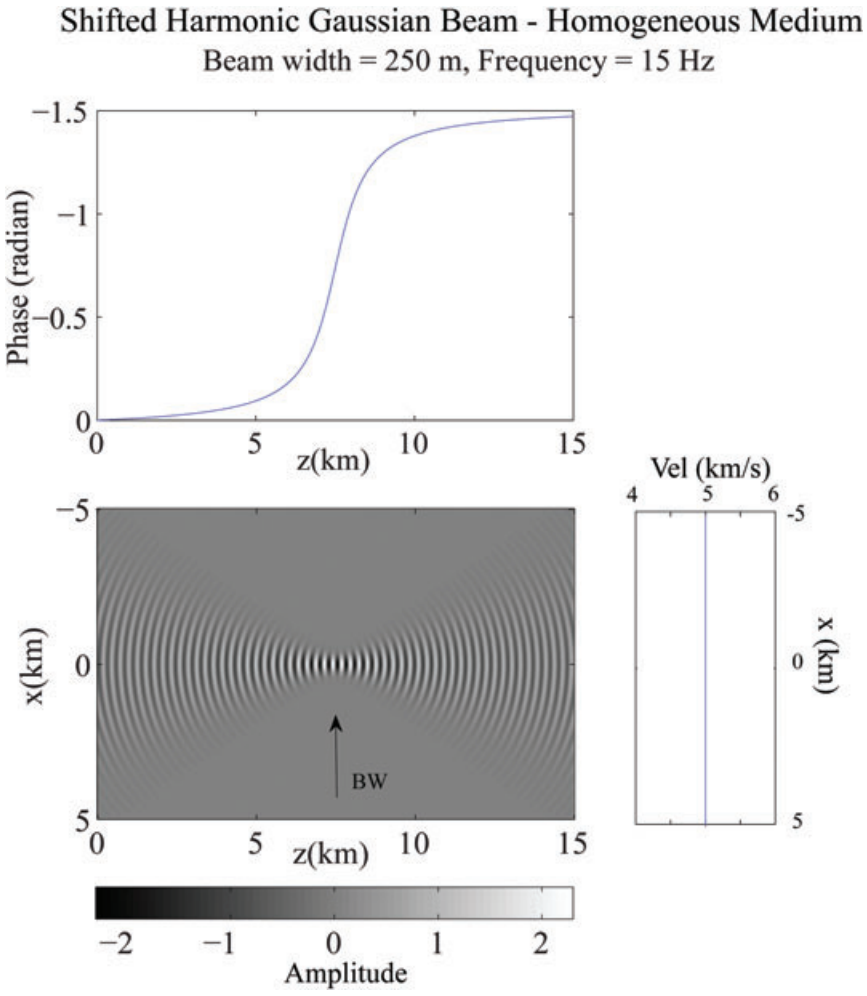

Figure 3. Harmonic Gaussian beam for a frequency of 15 Hz in a homogeneous medium. The beam-waist is located at 7.5 km with a beam-width of 250 m. The beam-field is shown at the bottom and the Gouy phase anomaly at the top. The beam-waist is indicated by BW.

et al. 1982) and is given by

$$\varepsilon = S_0 - iL_0^2, \tag{9}$$

where S_0 is the position of the beam-waist and $L(s_0) = \sqrt{\frac{2v_0}{\omega}} L_0$ specifies the beam-width. The position of the beam-waist determines where the planar part of the beam is located. ε is just one choice for the complex beam parameter and is equal to $1/M(s_0)$ where $M(s_0) = p(s_0)/q(s_0)$.

4 HARMONIC GAUSSIAN BEAMS IN HOMOGENEOUS MEDIA

For paraxial Gaussian beams in a homogeneous medium, the dynamic ray tracing can be solved analytically. In Fig. 1, an example is shown for a harmonic beam with a frequency of 15 Hz and a beam-waist located at $z = 0$ with a beam-width of 350 m. The background velocity is 5 km s^{-1} and the Rayleigh distance is 1.44 km. 'z' is now the propagation direction of the beam and 'x' is the transverse direction. The lower plot in Fig. 1 is the beam-field which is seen to spread with distance z. The top plot in Fig. 1 shows the Gouy phase anomaly which for the 2-D case reaches a value of $-\pi/8$ at the Rayleigh distance noted by RR in the plot. The remaining $-\pi/8$ is accumulated from the Rayleigh distance out to greater distances. For smaller initial beam-widths, the Rayleigh distance would be closer approaching $z = 0$, and more and more of the Gouy phase would be accumulated closer to the beam-waist. This would then give rise to the $-\pi/4$ phase shift for secondary wavelets used in the 2-D Huygens-Fresnel integral.

Fig. 2 shows a similar case with the beam-waist at $z = 0$, but now with a larger beam-width of 700 m. The beam is shown in the lower plot and spreads more slowly compared to the earlier example, now with a Rayleigh distance of 5.77 km. For this case the phase is not even up to $-\pi/4$ by 15 km at the right side of the model. Since this beam-width would be typical for Gaussian beams used for imaging in oil reservoirs, the Gouy phase anomaly would influence the beam calculations for all distances of interest for this application.

In Fig. 3, the beam-waist is now located in the centre of the model at 7.5 km noted by BW in the lower beam field plot and the beam-width at the beam-waist is 250 m. This shows that the Gouy phase anomaly is continuous across the beam-waist, with half resulting from the converging beam to the beam-waist and half from the beam diverging from the beam-waist. As the beam-width shrinks to zero, the Gouy phase anomaly in the limit would approach the discontinuous $-\pi/2$ phase jump for ray theory at a line caustic. The Gouy phase anomaly thus provides a continuous wave solution to explain the phase jump at caustics for ray theory.

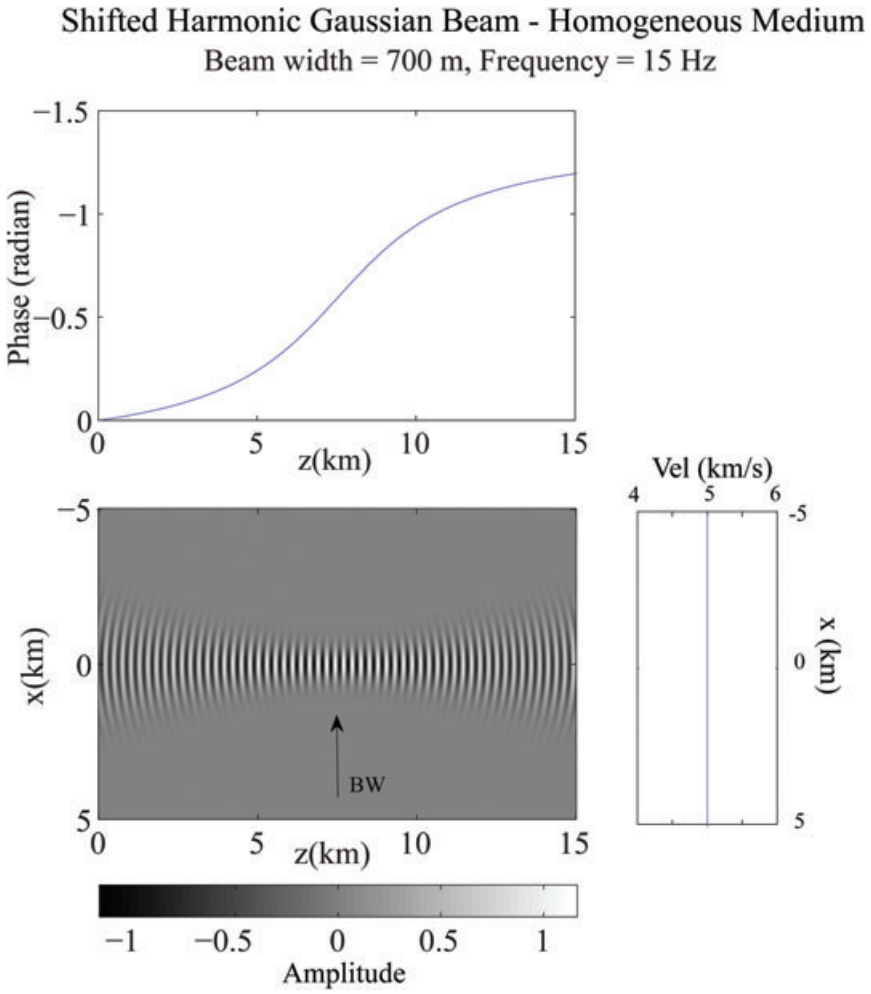

Figure 4. Harmonic Gaussian beam for a frequency of 15 Hz in a homogeneous medium. The beam-waist is located at 7.5 km with a beam-width of 700 m. The beam-field is shown at the bottom and the Gouy phase anomaly at the top. The beam-waist is indicated by BW.

In Fig. 4, a larger beam-width of 700 km is used with the beam-waist located at 7.5 km. The Gouy phase is now much more gradual over the entire propagation length of the beam. For this case, the complete $-\pi/2$ has still not accumulated over the 15 km of the model. Interestingly, as the beam-width gets larger, the Gouy phase flattens with propagation distance but influences a greater and greater propagation distance of the beam. Thus for very slightly confined or 'squeezed' plane waves, the Gouy phase will still be an important effect when considering large propagation distances.

5 HARMONIC GAUSSIAN BEAMS IN A QUADRATIC WAVEGUIDE

To investigate heterogeneous media, paraxial Gaussian beam solutions in a quadratic waveguide are now investigated. For given initial conditions, the dynamic ray equations can be solved either analytically or numerically by using the Runge-Kutta method. For the case of a quadratic velocity profile, the central ray along the waveguide will be a straight line, and a waveguide will be formed for a positive second derivative of the velocity in the x direction. The individual paraxial rays making up the beam solution will then fold back on themselves and form multiple focus points along the waveguide depending on the initial conditions.

Fig. 5 shows a Gaussian beam guided along the waveguide for a frequency of 15 Hz and an initial beam-width of 200 m. The beam-field is shown in the lower plot with two focus points along the z axis, each noted by BW. The upper plot displays the Gouy phase anomaly, which shows two flat areas separated by two areas of rapid phase advance associated with the beam focus locations. For the case of multiple focus points along the beam care needs to be taken to ensure that the phase is properly unwrapped to allow for a continuous phase advance with distance. For an isotropic media the Gouy phase anomaly will always be an advance, however, for anisotropic media there can be situations where the phase anomaly can decrease (Červený 2001; Chapman 2004).

In the example given in Fig. 5, the velocity is equal to $v(x) = v_0 + 0.5\, v_{22}(x - x_0)^2$ transverse to the beam, where $v_0 = 5$ km s^{-1} and $v_{22} = 1$. This results in a velocity at $x = \pm 2$ km of 7 km s^{-1}, and includes the transverse region over which the beam is mostly concentrated.

With a harmonic frequency of 15 Hz, the wavelength along the $x = 0$ axis is 0.33 km. The general validity condition for ray and paraxial methods are given by Červený (2001, pp. 607–609) and include that the wavelength $\lambda < a$, where 'a' is a characteristic scale of the medium. For a heterogeneous velocity medium with a quadratic profile, then $a \sim \frac{v}{|\nabla v|} = \frac{v_0}{|v_{22}(x-x_0)|}$. A second condition is $\lambda < a^2/L$, where L is the path length. This restricts the length of the path to not be too long because of the increase in size of the Fresnel zone with distance. For the example in Fig. 5, with $(x - x_0) = 2$ km, then for the first restriction, $\lambda = 0.33 < \frac{v}{|\nabla v|} \sim 2.5$. For the

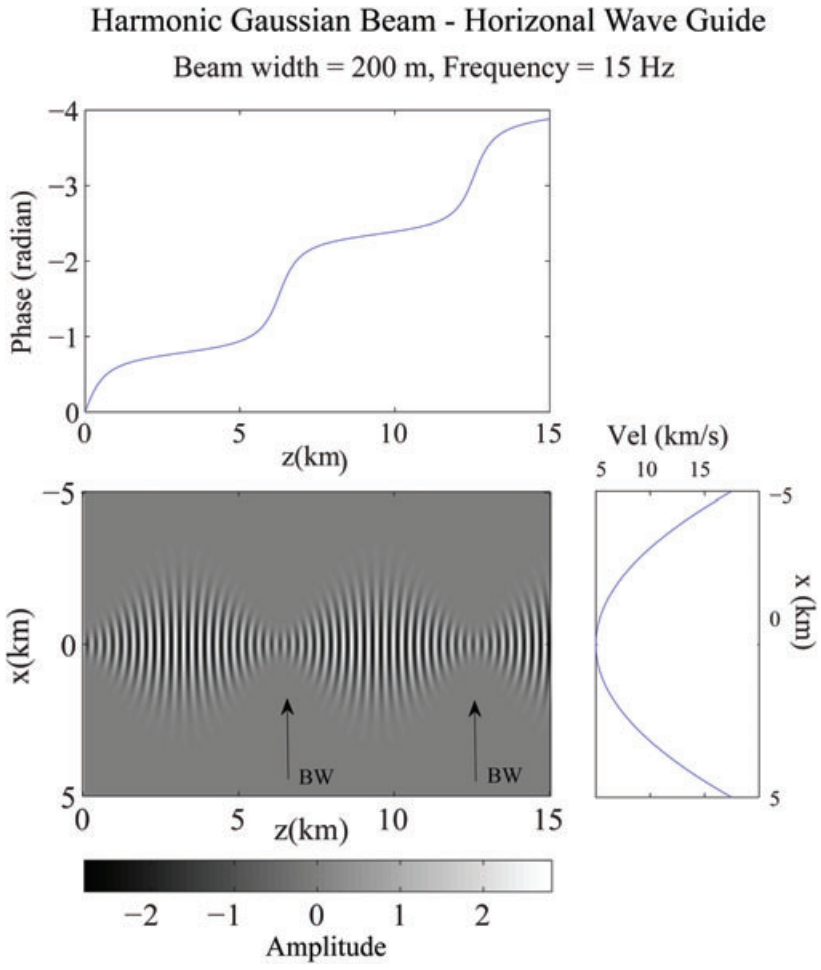

Figure 5. Harmonic Gaussian beam for a frequency of 15 Hz in a quadratic waveguide. The beam-waist $z = 0$ with a beam-width of 200 m. The beam-field is shown at the bottom where BW shows the beam focus locations. The Gouy phase anomaly is shown at the top.

second restriction, then $\lambda = 0.33 < [\frac{v}{|\nabla v|}]^2/L \sim 0.41$ for $L =$ 15 km. Although this second restriction is marginally satisfied for the largest distance, for most of the distance range in this example it is satisfied.

6 TIME-DOMAIN GAUSSIAN BEAMS IN HOMOGENEOUS MEDIA

To investigate time-domain beam solutions, the harmonic results for different frequencies are convolved with a Gabor wavelet, which can be written as

$$f(t) = \mathrm{e}^{-(2\pi f_M(t-t_i)/\gamma)^2} \cos(2\pi f_M(t - t_i) + \nu), \tag{10}$$

where f_M is the centre frequency and γ determines the number of wave cycles under the Gaussian envelope (Červený 2001). For the examples shown, $f_{\mathrm{M}} = 15\ Hz$, $\gamma = 3.5$ and $\nu = 0$.

In Fig. 6, the beam-waist is located at 7.5 km noted by BW in the lower beam-field plot with a beam-width of 200 m at the centre frequency. The time-domain traces at different z distances are shown in the top plot. The vertical line shows the predicted traveltimes $t = z/v$ for each centred Gabor wavelet, not accounting for the Gouy phase anomaly. An individual peak or trough on the traces can be seen to move to the left to earlier times as distance increases. In addition, there is a rapid increase in the phase advance between 6 and 9 km around the beam-waist. This slight advance in phase can be intuitively understood in terms of when a beam solution is confined or 'squeezed' at a focus, it slightly 'squirts' forward resulting in a change of pulse shape. However, this is a phase advance and not a group or energy advance and does not violate causality.

Fig. 7 shows a similar result, but now for a beam-width of 700 m at the centre frequency. Now the beam-field in the lower plot stays collimated for longer distances than in the previous example. The traces displayed in the top plot still show the time advance in the signals with distance, however, now the time advance is less abrupt at the focus distance.

Fig. 8 compares the results shown in Figs 6 and 7 with those computed using a second-order finite difference method. For both the narrow beam-waist of 200 m and the wide beam-waist of 700 m, two initial snapshots of the wavefield a time step apart are used as initial conditions for a modified code sufdmod2 from the package Seismic Unix (Cohen & Stockwell 2010). In Fig. 8 the solid lines are from the paraxial beam calculations and the dashed lines are from the finite difference calculations for different distance ranges. The vertical lines show the predicted traveltimes $t = z/v$ for each centred Gabor wavelet, not accounting for the Gouy phase anomaly.

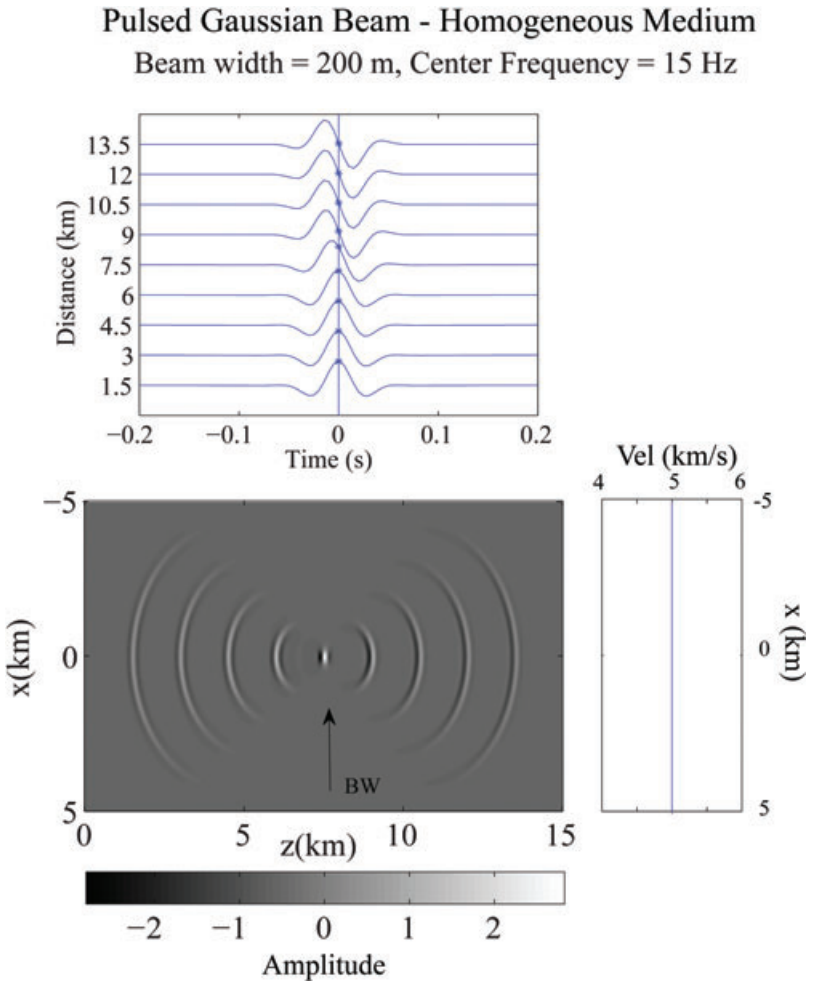

Figure 6. A time-domain Gaussian beam is shown using a Gabor wavelet for a centre frequency of 15 Hz and a $\gamma = 4$ in a homogeneous medium for the beam-waist located at 7.5 km with a beam-width of 200 m at the centre frequency. The beam-field is shown at the bottom and the time-domain traces for different z distances along the beam are shown at the top. The vertical line shows the predicted travel-times $t = z/v$ for each centred Gabor wavelet not accounting for the Gouy phase anomaly.

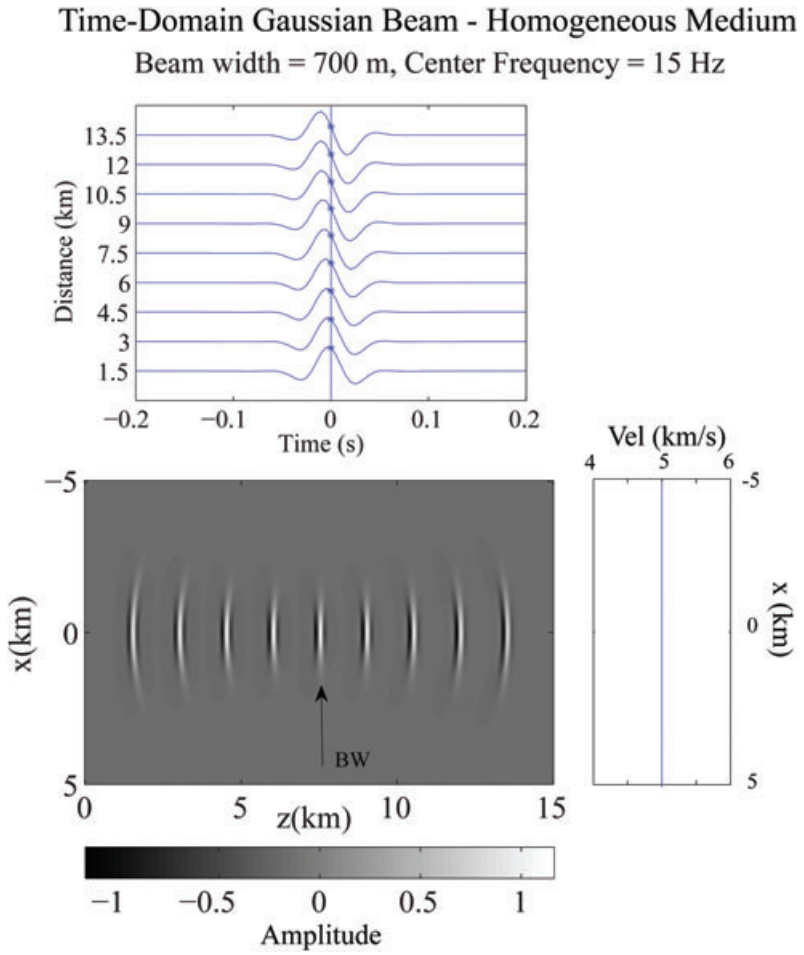

Figure 7. A time-domain Gaussian beam is shown using a Gabor wavelet with a centre frequency of 15 Hz and a $\gamma = 4$ in a homogeneous medium for the beam-waist located at 7.5 km with a beam-width of 700 m at the centre frequency. The beam-field is shown at the bottom and the time-domain traces for different z distances along the beam are shown at the top. The vertical line shows the predicted travel-times $t = z/v$ for each centred Gabor wavelet not accounting for the Gouy phase anomaly.

For both the paraxial beam and finite difference cases, the apparent phase advance of the pulse is observed.

All pulsed beam solutions will have a progressive phase advance with distance, which modifies the pulse shape. This could potentially influence the interpretation of traveltimes when using sources that generate beamed signals, for example from transducer sources in the laboratory. Note, however that the phase advance described here will primarily affect the pulse shape but could influence the picking of traveltimes when using correlation approaches for beamed signals.

7 CONCLUSION

In this paper, we have illustrated the Gouy phase anomaly using harmonic and time-domain Gaussian beams, where the Gouy phase affects all spatially confined solutions to the wave equation. For harmonic Gaussian beams, the Gouy phase anomaly varies continuously with distance. This is in contrast to ray solutions, which have discontinuous phase anomalies at caustic points which are counted using the KMAH index. However, as the beam-width at a focus point gets smaller, the Gouy phase anomaly for beams will concentrate around the focus point and approach the discontinuous phase jump at a caustic for ray solutions. The propagation of Gaussian beams in heterogeneous media is illustrated using a quadratic velocity waveguide, where multiple focus points for beams can be generated. However, care must be taken to ensure that the phase is properly unwrapped to allow for a continuous Gouy phase anomaly with distance.

Finally, time-domain Gaussian beams have been investigated using a Gabor wavelet. The traveltimes of the time-domain signals are slightly advanced by the Gouy phase anomaly at focus points of a beam. Intuitively this can be understood in terms of when a wave solution gets 'squeezed' at a focus, it 'squirts' forward slightly in phase and increases its apparent speed in the propagation direction resulting in a change of pulse shape. However, this a phase advance and not a group or energy advance and does not violate causality. Nonetheless, this could be important for interpreting traveltimes when pulse shapes change for experiments using beamed signals, such as from transducers in the laboratory. It will also have an effect when using Gaussian beams and other confined wave solutions for seismic imaging.

ACKNOWLEDGMENTS

This work was supported in part by the National Science Foundation grant EAR06-35611 and the U.S. Air Force contract FA8718-08-C-002 and partly by the members of the Geo-Mathematical Imaging Group (GMIG) at Purdue University.

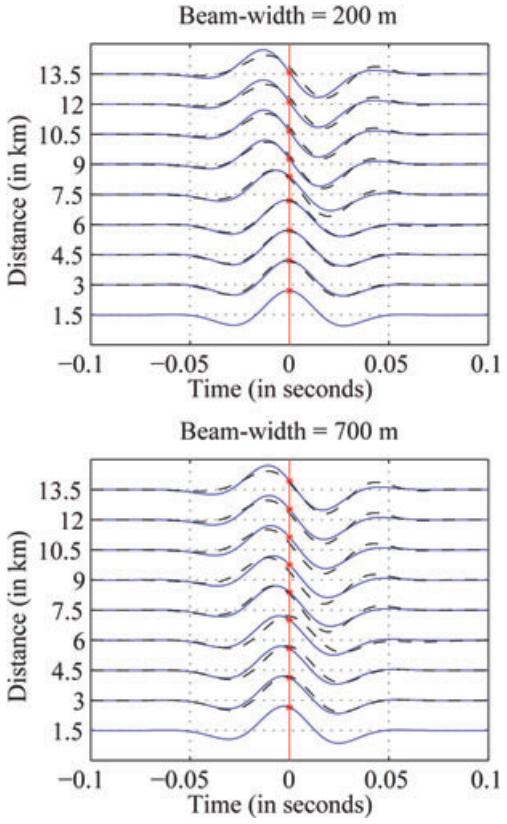

Figure 8. This shows a comparison between the time-domain paraxial Gaussian beams and those derived using the explicit second-order finite difference method. The top plot shows the comparison for the narrow beam case with the beam-width equal to 200 m at the beam-waist given in Fig. 6 and the bottom plot shows the comparison for the wide beam case with the beam-width equal to 700 m at the beam-waist. In both plots, the solid line is the paraxial Gaussian beam solution and the dashed line is the finite difference solution.

REFERENCES

Aki, K. & Richards, P.G., 2002. *Quantitative Seismology,* 2nd edition, University Science Books, Sausalito, California.

Arnold, V.I., 1967. Characteristic classes entering in quantization conditions, *Funct. Anal. Appl.,* **1,** 1–13.

Boyd, R.W., 1980. Intuitive explanation of the phase anomaly of focused light beams, *J. Opt. Soc. Am.,* **70,** 877–880.

Červený, V., 2001. *Seismic Ray Theory,* Cambridge University Press, Cambridge.

Červený, V., Popov, M.M. & Pšenčík, I., 1982. Computation of wavefields in inhomogeneous media–Gaussian beam approach, *Geophys. J. R. astr. Soc.,* **70,** 109–128.

Chapman, C.H., 2004. *Fundamentals of Seismic Wave Propagation,* Cambridge University Press, Cambridge.

Chew, W.C., 1990. *Waves and Fields in Inhomogeneous Media,* Van Nostrand Reinhold, New York.

Cohen, J.K. & Stockwell, J.W.Jr., 2010. CWP/SU: Seismic Un∗x Release No. 4.2: an open source software package for seismic research and processing, Center for Wave Phenomena, Colorado School of Mines.

Deschamps, G.A., 1971. Gaussian beam as a bundle of complex rays, *Electr. Lett.,* **7,** 684–685.

Felsen, L.B., 1976. Complex-source-point solutions of the field equations and their relation to the propagation and scattering of Gaussian beams, *Ist. Naz. Alta Matem. Symp. Math.,* **18,** 39–56.

Feng, S. & Winful, H.G., 2001. Physical origin of the Gouy phase shift, *Opt. Lett.,* **26,** 485–487.

Gouy, G., 1890a. Sur une propriété nouvelle des ondes lumineuses, *Compt. Rendue Acad. Sci. (Paris),* **110,** 1251–1253.

Gouy, G., 1890b. Sur la propagation anomale des ondes, *Compt. Rendue Acad. Sci. (Paris),* **111,** 33–35.

Hormander, L., 1971. Fourier integral operators, *Acta Math.,* **127,** 79–183.

Keller, J.B., 1958. Corrected Bohr-Sommerfeld quantum conditions for non-separable systems, *Ann. Phys.,* **4,** 180–188.

Kravtsov, Yu.A. & Berczynski, P., 2007. Gaussian beams in inhomogeneous media: a review, *Studia Geophys. et Geod.,* **51,** 1–36.

Kravtsov, Yu. A. & Orlov, Yu. A., 1990. *Geometrical optics in inhomogeneous media,* Springer-Verlag, Berlin.

Maslov, V.P., 1965. *Theory of Perturbations and Asymptotic Methods,* Moscow State Univ. Press, Moscow (in Russian).

Nowack, R.L. & Aki, K., 1984. The two-dimensional Gaussian beam synthetic method: testing and application, *J. geophys. Res.,* **89,** 7797–7819.

Popov, M.M., 1982. A new method of computation of wave fields using Gaussian beams, *Wave Motion,* **4,** 85–97.

Popov, M.M., 2002. *Ray Theory and Gaussian Beam Method for Geophysicists,* Lecture notes University of Bahia, Salavdor, Brazil.

Siegman, A.E., 1986. *Lasers,* University Science Books, Mill Valley, CA.

Simon, R. & Mukunda, N., 1993. Bargmann invariant and the geometry of the Gouy effect, *Phys. Rev. Lett.,* **31,** 880–883.

Subbarao, D., 1995. Topological phase in Gaussian beam optics, *Opt. Lett.,* **21,** 2162–2164.